

Electrochemical and Quantum Chemical Studies of 1, 5-bis (2-nitrophenyl)-1, 4-pentadien-3-one as Corrosion Inhibitors for Mild Steel in Hydrochloric Acid Solution

R. Sasi kumar¹, R.Karthik¹, Shen-Ming Chen^{1,*}, P.Prakash², P. Muthukrishnan^{3,*}, K.Shankar³, A.Kathiresan³

¹ Department of Chemical Engineering and Biotechnology, National Taipei University of Technology, Taipei, Taiwan 106 (ROC)

² PG and Research Department of Chemistry, Thiagarajar college, Madurai-625009, India.

³ Department of Chemistry, Faculty of Engineering, Karpagam University, Coimbatore-641021, India.

*E-mail: Smchen78@ms15.hinet.net, mukepmk@gmail.com

Received: 8 July 2016 / Accepted: 29 August 2016 / Published: 10 October 2016

Effects of 1, 5-bis (2-nitrophenyl)-1, 4- pentadien -3-one (BPDO) on mild steel in 1M hydrochloric acid solutions were explored using weight loss and electrochemical techniques. Mass losses of polished mild steel in 1M HCl measured after diverse time exposure of 2-24h show that the presence of BPDO drastically decreases the rate of mild steel dissolution and the effect enhances upon increasing its concentration. Potentiodynamic polarization experiments demonstrate a large diminish in cathodic, anodic and corrosion currents due to the presence of BPDO in 1M hydrochloric acid. The increase in adsorption of the BPDO on the mild steel surface and reduce of mass transport in the presence of BPDO upon increasing its concentration were confirmed by Electrochemical Impedance spectroscopy (EIS) measurements. The adsorption of BPDO abide Langmuir adsorption model. Activation parameters such as activation energy, enthalpy of activation and entropy of activation were calculated and discussed. Quantum chemical studies were performed to correlate BPDO efficiency and their molecular structure using quantum chemical calculations.

Keywords: Anticorrosion, Corrosion Inhibitor, Electrochemical Impedance spectroscopy, SEM, EDX, Adsorption

1. INTRODUCTION

The protection of metal from corrosion is the major problem faced by the industries. One of the effective way to control corrosion is by using corrosion inhibitors. During the last past decades, using

organic compounds as effective inhibitors to inhibit corrosion of mild steel in acid solutions [1-3]. Corrosion inhibitors, mostly act in accordance with the adsorption levels of their respective molecules on any metal surface. The metal's nature and surface change, its medium and the inhibitors chemical structure are the factors that influence their action [4]. Several authors have reported the use of many organic compounds such as schiff base [5], azoles [6], 2, benzylaminopurine [7], thiophene derivatives [8], pyrazole derivatives [9] pyrimidine derivatives [10-12], pyridine derivatives [13] and bipyrazole derivatives [14] in acidic media as efficient corrosion inhibitors for steel. It is commonly observed that formation of an inhibitor- iron complex on a metal surface is promoted by an organic inhibitor. This process is achieved by the formation of a covalent bond by moving electrons from the organic compounds to the metal during the cause of chemical adsorption. Here it is proved that the metal plays the role of an electrophile. It is also made clear that the electron rich centers of the organic molecule supplemented with lone pairs of electron that are promptly available for distribution in the formation of a bond. Dibenzalacetone derivatives are great interest due to their potential activity against bacterial, cancer, antitumoral, antimetabolic, chemoprotective, anti-inflammatory, antimicrobial, anti-nociceptive and antifungal infections. The choice of the 1, 5-bis (2-nitrophenyl)-1, 4- pentadien -3-one as corrosion inhibitor is based on two ways: it can be easily prepared from low cost material, the presence of delocalized pi-electron on the two benzene ring with an unsaturated chain, active functional groups such as nitro (-NO₂) and carbonyl (-C=O) group, which can influence the positive adsorption of the inhibitor molecule onto the surface of mild steel. Nonetheless, there is no work done on the use of 1, 5-bis (2-nitrophenyl)-1, 4- pentadien -3-one (BPDO) on mild steel in hydrochloric acid. The anticorrosive activity of BPDO on mild steel was investigated through non electrochemical and electrochemical tools such as mass loss measurements, X-ray diffraction studies (XRD), Fourier transform infrared spectroscopy (FT-IR), Scanning electron microscopy (SEM), Energy dispersive X-ray spectroscopy (EDX), potentiodynamic polarization techniques and electrochemical impedance spectroscopy (EIS). Additionally, thermodynamic and quantum chemical parameters were calculated and discussed.

2. EXPERIMENTAL

2.1. Specimens and Solutions Preparation

Mass loss tests were carried out on mild steel specimen of chemical composition: C-0.05 %, Mn-0.6%, P- 0.36%, Si-0.03% and the remainder iron. Mild steel specimens were used in the sheet form of 2.5 cm × 2.5 cm × 0.4 cm dimensions. Before mass loss test, mild steel specimens were cleaned with acetone, dried and stored moisture free desiccators. AR grade hydrochloric acid and double distilled water were used to prepare 1M HCl solution for all corrosion tests. BPDO was synthesized based on the literature procedure as earlier reported [15]. The concentration range of BPDO employed was 100 mg/l – 300 mg/l in 1M HCl solutions. The molecular formula of the BPDO is C₁₇H₁₂N₂O₅ and its chemical structure is given in Fig.1.

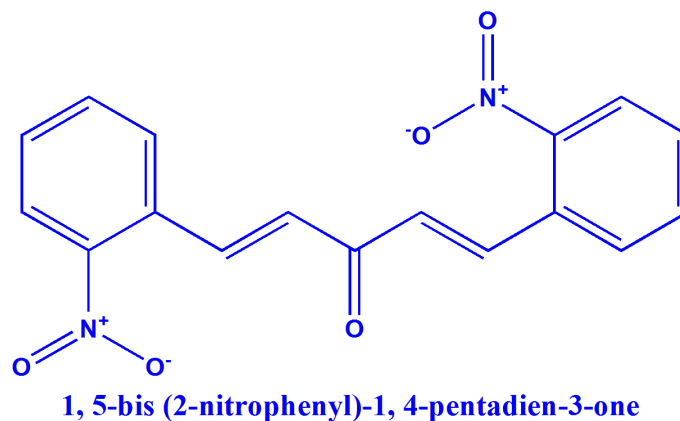


Figure 1. Chemical structure of BPDO

2.2. Mass Loss Method

Mass loss is one of the easiest and widely used techniques of preliminary inhibition assessment. The pre-weighted and polished mild steel sheet exposed in 100 ml of 1M HCl solution without and with various concentrations of BPDO at 308-328K for 2 h. After 2 h, the sheet were taken from the solution, washed with double distilled water, rinsed with acetone, dried and reweighed. The mass of each steel sheet before and after immersion was evaluated using an analytical balance. Tests were done in triplicate at the same time, and the mass losses averaged. The mass loss (ΔM) was used to determine the corrosion rate (CR) and the inhibition efficiency (% IE):

$$\text{CR (mpy)} = 534 \times \Delta M / D \times S \times T \quad (1)$$

$$\text{IE \%} = (M_0 - M_i) / M_0 \times 100 \quad (2)$$

Here $\Delta M = (M_0 - M_i)$, where M_i and M_0 are the mass loss of mild steel in the presence and absence of BPDO respectively, S is the size of the sheet in cm^2 , D is the density of the iron (g/cm^3), T is the time of immersion in hours.

2.3. Electrochemical Method

Tafel polarization curves and Nyquist curves were recorded using CH electrochemical analyzer Model 604D. A mild steel sheet surrounded in araldite with uncovered area of 0.5cm^2 was used as a working electrode. A platinum electrode and saturated calomel electrodes were used as a counter electrode and reference electrode. All electrochemical measurements were performed at 308K using 100ml of 1M HCl solution without and with various concentrations (100 mg/l – 300 mg/l) of BPDO. Before recording of the Tafel polarization curves and electrochemical impedance study, the electrode was exposed in 1M HCl solution for 1800 sec to attain a steady state. Tafel polarization curves were recorded from negative to the positive direction ($\text{OCP} \pm 300 \text{ mV}_{\text{SCE}}$) with a scan rate of 1 mV/sec and the parameters such as corrosion current density (j_{corr}), Tafel anodic slope (b_a), cathodic slope (b_c) and corrosion potential (E_{corr}) were calculated. From j_{corr} , the inhibition efficiency was calculated by using the formula:

$$IE\% = \frac{(j_{\text{corr (blank)}} - j_{\text{corr (inhibitor)}})}{j_{\text{corr (blank)}}} \times 100 \quad (3)$$

Where $j_{\text{corr (blank)}}$ and $j_{\text{corr (inhibitor)}}$ are the corrosion current density in absence and presence of different concentrations of inhibitor respectively. EIS measurements were performed at OCP in the frequency range of 0.1 Hz to 100 KHz using ac voltage. Impedance parameters such as double layer capacitance (C_{dl}) and charge transfer resistance (R_{ct}) values were calculated from nyquist plot. Inhibition efficiency was calculated using the equation:

$$\% IE = \frac{(R_{ct} - R_{ct}^0)}{R_{ct}} \times 100 \quad (4)$$

Where R_{ct} and R_{ct}^0 are values of charge transfer resistance in presence and absence of BPDO respectively. Each experiment was done at triplicate to check the accuracy of the data.

2.4. XRD analysis

The polished mild steel sheet was immersed in 1M HCl solution without and with maximum concentration (300 mg/l) of BPDO for 2 h. Then, they were taken out and dried. The nature of the protective layer adsorbed on the surface of the mild steel sheet was examined by using XRD-Gonimeter, (SHIMADO-Model XRD 6000).

2.5. FT-IR studies

The spectra for BPDO as well as the BPDO adsorbed on mild steel surface were confirmed by FT-IR spectroscopy (SHIMADZU- FTIR- 8400S spectrophotometer).

2.6. SEM and EDX analysis

The mild steel sheet used for composition and surface morphology examination immersed in 1M HCl solution containing 300 mg/l of BPDO and 1M HCl for 2h. After 2 h, the mild steel sheet was removed, rinsed with acetone and dried. The analysis was carried out using EDX technique (INCA penta FETX3 instruments) and SEM technique (JSM 6390 JEOL).

2.7. Computational Studies

Theoretical calculations were carried out using density functional theory (DFT) with Gaussian 09W program for basis set for all atoms in BPDO molecules. The molecular structure and electronic properties of BPDO have completely and geometrically optimized. The quantum chemical parameters such as energy of the highest occupied molecular orbital (E_{HOMO}), energy of the lowest unoccupied molecular orbital (E_{LUMO}), dipole moment (D), energy gap (ΔE) was determined.

3. RESULTS AND DISCUSSION

3.1. Mass Loss Measurements

The protection efficiency and corrosion rate of mild steel immersed in 1M HCl without and with various concentrations of BPDO at 308 K (Figure 2). From the Fig.2, it can be seen that the increase in BPDO concentration inhibition efficiency increases and reduces the corrosion rate of mild steel. This behavior could be attributed by the formation of protective layer by the adsorption BPDO molecules on mild steel surface. The maximum efficiency is found to be 98.91% in 1M HCl solution at higher concentration of 300 mg/l at 308K. No appreciable change was found on further increase in the inhibitor concentration. The reason for higher inhibition efficiencies of the BPDO towards mild steel may be due to the presence of active functional group such as NO₂ group, carbonyl and pi-electrons in the BPDO molecules. In order to study the effect of temperature on the corrosion behavior of mild steel sheet were exposed in 1M HCl solution containing different concentrations of the BPDO at 308 to 328K.

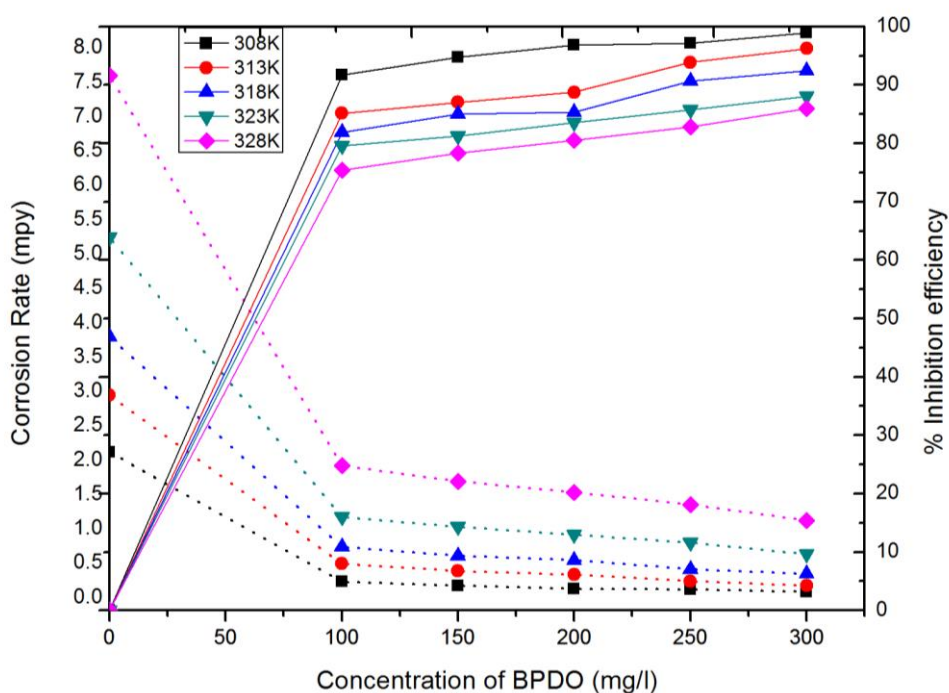


Figure 2. Inhibition efficiency and corrosion rate of mild steel specimens exposed in 1M HCl in the presence and absence of BPDO at 308, 313, 318, 323, 328K; (dashed line) inhibition efficiency; (dotted line) corrosion rate

The calculated values of inhibition efficiency and corrosion rate are given in Figure 2. As the temperature increases, the inhibition efficiency decreased and the corrosion rate values increased. This could have arisen by the inhibitive film formed on mild steel surface was less protective indicating that the desorption of BPDO molecules from surface of mild steel at higher temperatures [16]. Fig 3

illustrates the deviation of inhibition efficiency as a function exposure time at 308K. The results showed that protection efficiency of BPDO improved as the concentration of BPDO rose from 100 mg/l to 300 mg/l. Beyond 300 mg/l, it causes a low degree of protection. The optimum concentration of BPDO was found to be 300 mg/l. It is evident from the figure that protection efficiency diminished with raise in the exposure time from 2 to 24h indicating the instability of BPDO film on the metal surface up to 24h [17]. At higher temperature, inhibition efficiency of BPDO was found to decrease with the increase in temperature demonstrating that desorption of insulated film of BPDO from mild steel surface [18].

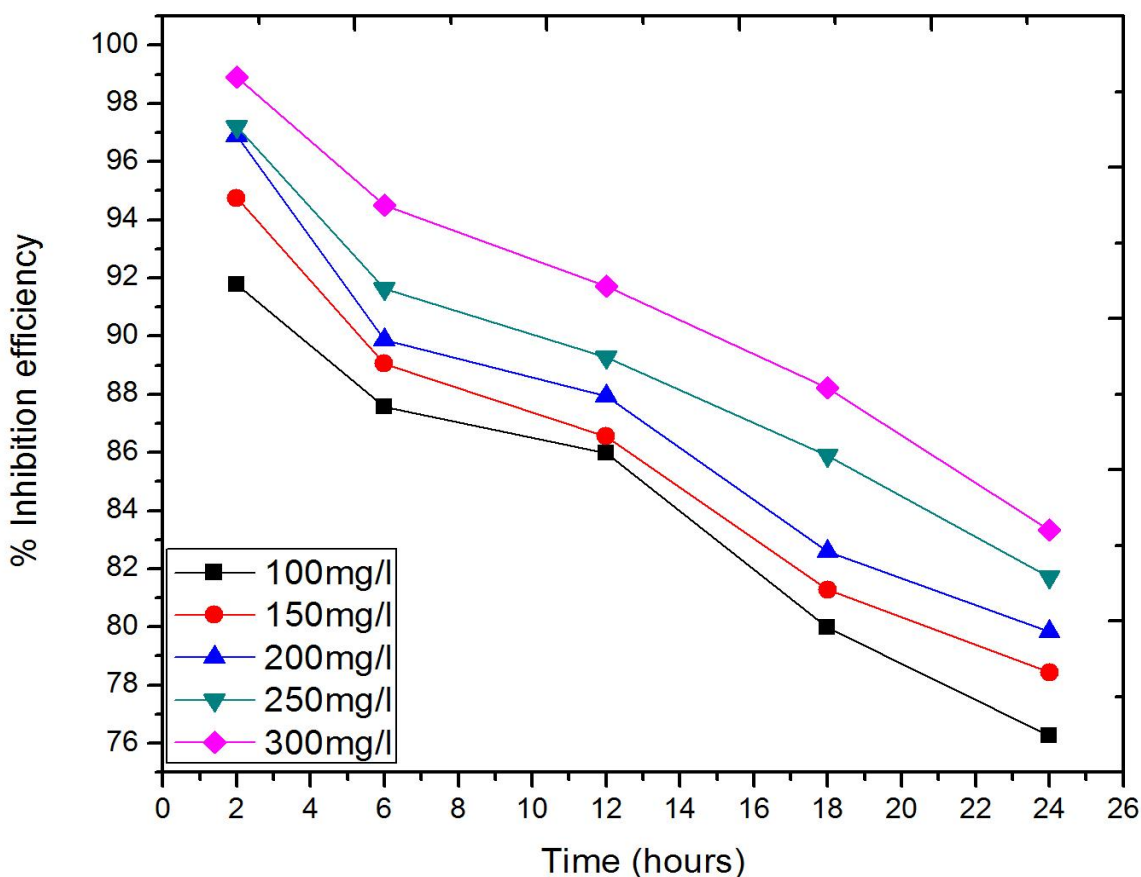


Figure 3. Effect of exposure time on the protection efficiency of BPDO at 308K.

3.2. Thermodynamic Activation Parameters

The effect of temperature on the rate of electrochemical corrosion of metal is an important scientific and industrial topic. In acid solution, CR increases exponentially with raise in temperature. Usually corrosion reactions are regarded as Arrhenius processes and the CR can be expressed as follows:

$$\log CR = \log A - (E_a/2.303RT) \tag{5}$$

Here E_a is the apparent activation energy, A is the frequency factor, R is the molar gas constant ($8.314 \text{ JK}^{-1}\text{mol}^{-1}$) and T is temperature. The activation energy (E_a) at various concentrations of BPDO was calculated by linear regression between $\log(\text{CR})$ and $1/T$ in 1M HCl is shown in Fig 4. In 1M HCl solution, the activation energy (E_a) of the corrosion inhibition process increases to great extent in the presence of BPDO compared to uninhibited solution. The physical adsorption taking place in the first stage is understood as the increase in the E_a [19]. We note the decrease in adsorption results in the increase of desorption of inhibitor molecules because these two antithetical processes are in the state of equilibrium. Because of the increase in desorption of inhibitor molecules at higher temperatures, the large surface area of mild steel comes into contact with aggressive environment. This results in proportionate increase of the corrosion rate with the increase in temperature. Our experimental data demonstrate that the decrease of inhibition efficiency value with increase of temperature and the higher value of E_a in presence of BPDO inhibitors can be interpreted as physisorption. In general, the presence of both electrically charged surface of the mild steel and changed ions in the bulk of the solution are required for the process of physical adsorption to take place. As the requirement for a transition metal is not fulfilled, it is essential to have a low energy electron orbital and inhibitor molecules with loosely bound electrons or heteroatoms with lone pair of electrons. However, the substances studied are BPDO adsorbs electrostatically on mild steel surface through lone pair of electrons in oxygen and pi electrons in the BPDO molecules.

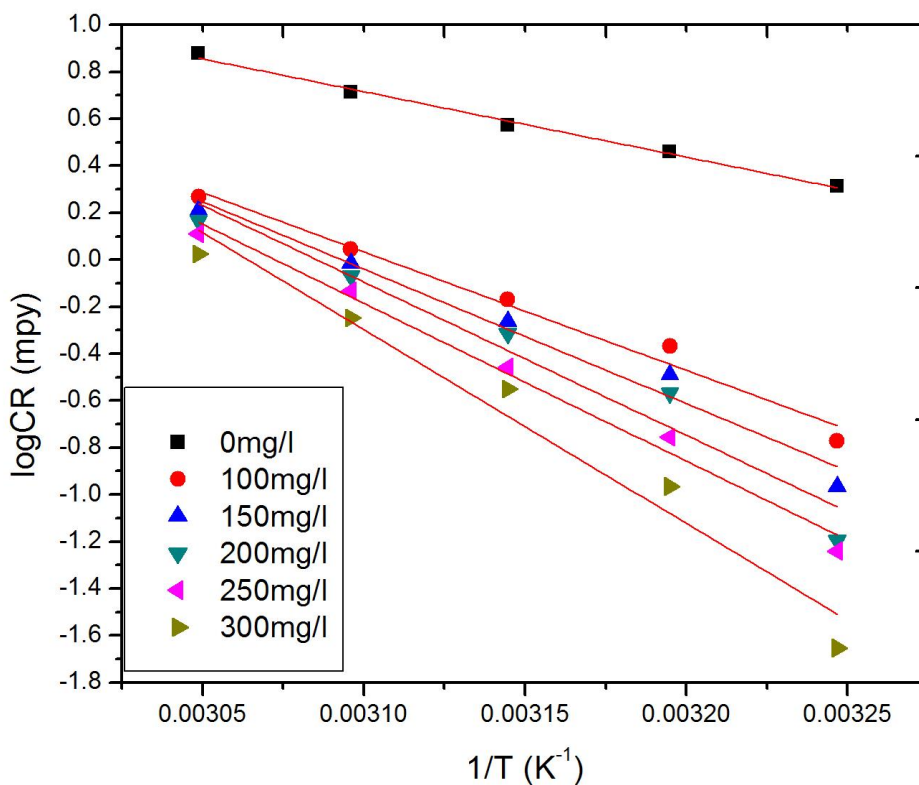


Figure 4. Arrhenius plots for CR mild steel in 1M HCl with and without inhibitor

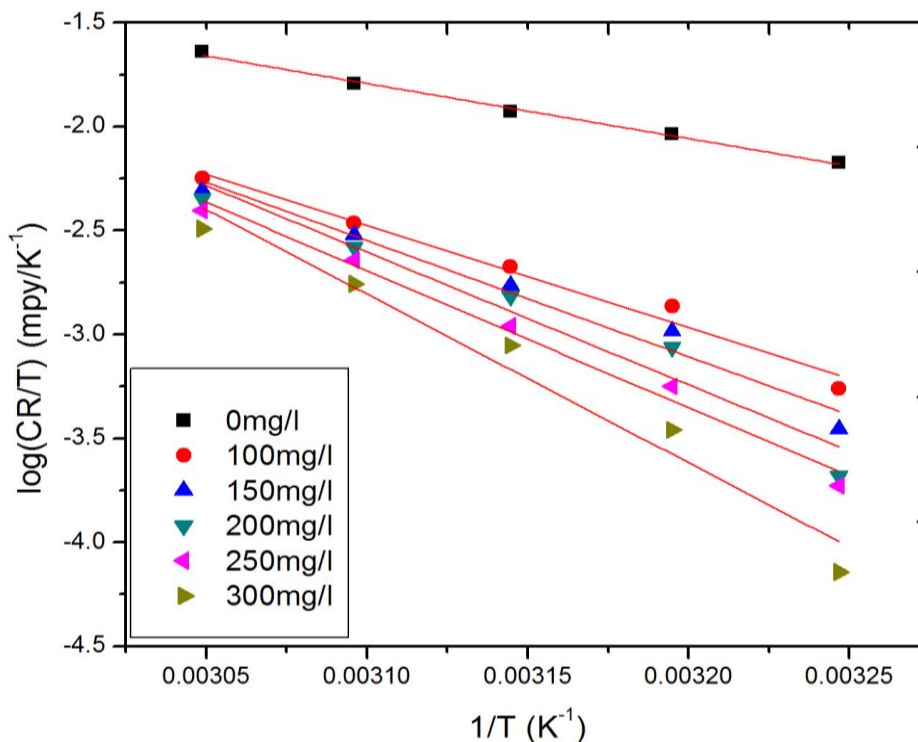


Figure 5. Transition state plots for CR of mild steel in 1M HCl with and without inhibitor

The enthalpy activation (ΔH_a) and entropy of activation (ΔS_a) were calculated by the transition state equation:

$$\log CR/T = \{\log(R/hN) + (\Delta S_a/2.303R)\} - (\Delta H_a/2.303RT) \tag{6}$$

Here N is Avogadro’s number and h is plank’s constant. Fig.5 shows plots of log (CR/T) versus 1/T for 1M HCl in presence of BPDO. Straight lines were obtained with a slope ($\Delta H_a = -\text{slope}/2.303R$) and an intercept of $\log(R/Nh + \Delta S_a/2.303R)$ from which the values of ΔH_a and ΔS_a are calculated and are given in Table 1.

Table 1. Activation parameters of mild steel in 1M HCl solutions in the absence and presence of different concentrations of BPDO

Concentrations of BPDO (mg/l)	E_a (kJ/mol)	ΔH^* (kJ/mol)	ΔS^* (J/mol/K)
0	53.40	50.76	-74.49
100	96.65	94.012	46.36
150	109.84	107.20	85.99
200	124.99	122.35	131.75
250	128.84	126.19	142.09
300	158.17	155.53	230.74

We report the positive sign of ΔH_a reflect the endothermic nature of the mild steel dissolution process. It also suggests that in the presence of inhibitors, the rate of dissolution of mild steel is slow [20]. It is understood from the positive values of the entropy of activation that the system passes from

less orderly to a more random rearrangement in the presence of the inhibitor. In other words, dissociation rather than association is the result of activated complex in the rate determining step that means disordering increases going from reactants to the activated complex [21-23].

3.3. Potentiodynamic polarization studies

In optic to get more information about the nature of a organic compound for anodic, cathodic or mixed type inhibitor, the polarization behavior of mild steel were studied at 308K in the absence and presence of various concentrations of the BPDO as shown in Fig.6. In the presence of BPDO, the curves are shifted to lower current regions indicates that the inhibition tendency of the BPDO.

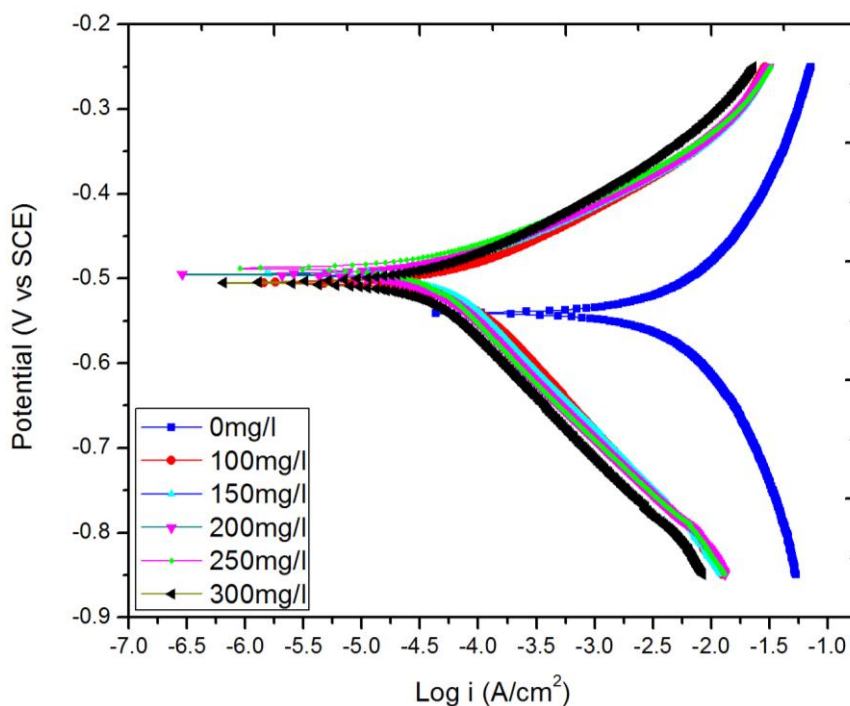


Figure 6. Polarization curve for mild steel containing different concentrations of BPDO in 1 M HCl

Table 2 shows the polarization parameters such as current density (j_{corr}), corrosion potential (E_{corr}), Tafel anodic and cathodic slope (b_a , b_c) obtained by extrapolation of the Tafel lines. The results suggested that the addition of the BPDO in 1M HCl solution retards both anodic dissolution and hydrogen evolution reaction of mild steel electrode. The maximum inhibition efficiency found to be 99.29% at an optimum concentration of 300 mg/l. From the inspection of data given in Table 2, it is clear that in the presence of inhibitor the value of corrosion current density (j_{corr}) is lower than in free acid solutions. In the presence of various concentrations of BPDO, there was no significant change in the shift of corrosion potential values after the addition of BPDO. But slight change is noted in the values of b_c in the presence of BPDO, whereas very noticeable change occurs in the values of b_a . This result indicates that suppressed anodic reactions and also reduces cathodic reactions but the more

predominant effect on the anodic reactions. It is to conclude that though BPDO acted as mixed type corrosion inhibitors, the more predominant were anodic inhibitors.

Table 2. Potentiodynamic polarization parameters for the corrosion of mild steel in 1M HCl solutions containing different concentrations of BPDO

$C_{inh}(mg/l)$	$-E_{corr}$ (mV)	j_{corr} ($\mu A\ cm^{-2}$)	$-b_c$ (mV/decade)	$-b_a$ (mV/decade)	% IE
0	541	5700	183.21	172.68	-
100	505	72.07	146.13	73.551	98.73
150	494	65.75	145.03	69.276	98.84
200	485	48.04	142.97	67.091	99.15
250	488	44.31	143.16	66.233	99.22
300	505	40.45	139.91	75.041	99.29

3.4. Electrochemical Impedance Spectroscopy

A significant increase in the impedance system causing enhance in the resistance to charge transfer process is the result as formation of an insulated layer on the mild surface. It is obvious that the measurements of the impedance spectroscopy determine the performance of an inhibitor. Electrochemical impedance spectra for the corrosion behavior of mild steel in 1M HCl in absence and presence of inhibitor are depicted in Fig 7. These plots having the shape of a semicircle for all the concentrations of BPDO examined indicate that the corrosion is mainly inhibited by charge transfer process. The electrochemical impedance parameters namely the solution resistance (R_s), charge transfer resistance (R_{ct}) and double layer capacitance (C_{dl}) are derived from these curves are given in Table 3. Inspection of the table shows that the R_{ct} increases from the value of $4.05\Omega/cm^2$ for the blank to $272.16\Omega/cm^2$ for the higher concentration of BPDO providing 98.51% inhibition efficiency. It could be observed that the R_{ct} increased with increase in the concentration of BPDO signifies that the insulated film obtained acts as a barrier layer to the corrosion process that clearly proves the existence and formation of the film [24]. The C_{dl} values are also used to calculate the surface coverage θ using the relationship:

$$\theta = \frac{(C_{dl} - C_{dl}^i)}{C_{dl}} \tag{7}$$

Here C_{dl}^i and C_{dl} are the double layer capacitance values in the presence and of absence inhibitors. The values of double layer capacitance (C_{dl}) decrease from $2.51 \times 10^{-2} F/cm^2$ for the blank to $6.13 \times 10^{-6} F/cm^2$ for 300mg/l BPDO. With the increase in BPDO concentration, the decrease in C_{dl} at the interface of an electrode and electrolyte was due to the strong adsorption of BPDO molecules at the interface, since according to electrochemical theory a decrease in C_{dl} is proportional to the adsorption rate [25].

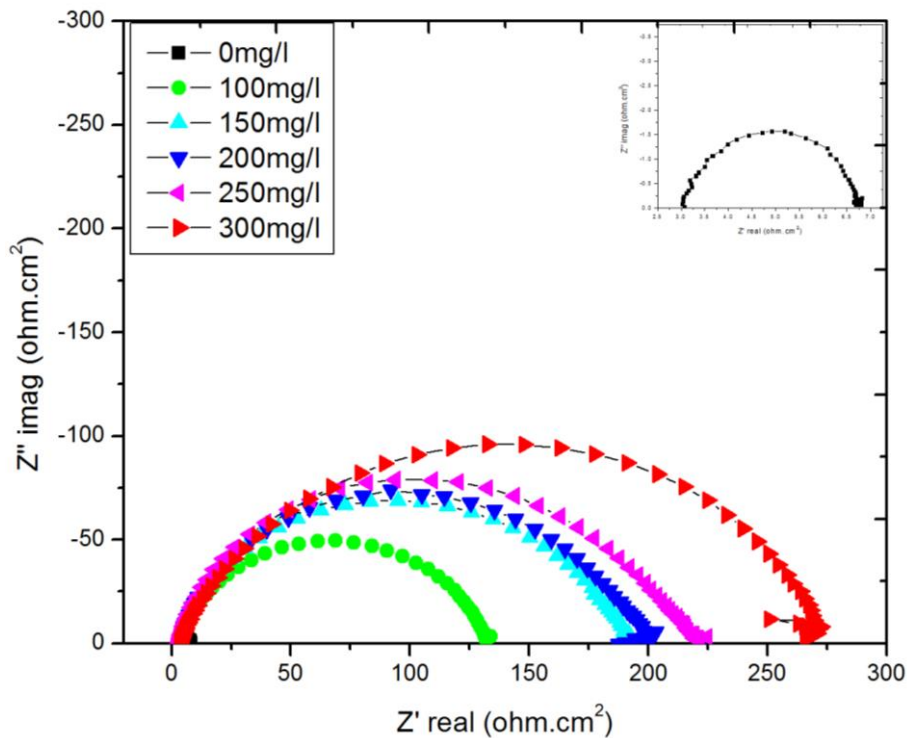


Figure 7. Impedance curves of BPDO on mild steel in 1M HCl with and without BPDO.

Table 3. Electrochemical impedance parameters for mild steel in 1M HCl solutions in the absence and presence of BPDO

$C_{inh}(mg/l)$	$R_s(\Omega cm^2)$	$R_{ct}(\Omega cm^2)$	$C_{dl}(F/cm^2)$	% IE
0	2.921	4.05	2.51×10^{-2}	-
100	2.781	128.51	2.50×10^{-5}	96.84
150	2.240	186.66	1.24×10^{-5}	97.83
200	2.632	188.46	1.15×10^{-5}	97.85
250	2.596	216.00	9.37×10^{-6}	98.12
300	2.640	272.16	6.13×10^{-6}	98.51

3.5. Adsorption isotherm

The adsorption of organic inhibitor molecules at the metal surface is the initial step in inhibition of metallic corrosion. The adsorption is dependent on the molecular area, molecular mass of the inhibitor. the presence of functional groups such as -N=N, R-OH, -CHO etc, temperature, electronic structure of inhibiting molecules, steric factor, aromaticity and electron density at donor site and electrochemical potential [26-29]. It is obvious that, at metal/solution interface, the solvent H₂O molecules could also involve in the act of adsorption. And so the process of adsorption of an organic adsorbate from the aqueous solution on to metal-solution interface was expressed as quasi-substitution

process that takes place between water molecules at the metal surface [$\text{H}_2\text{O}(\text{ads})$] and the organic compounds in the aqueous phase [$\text{Org}(\text{sol})$].



Where $\text{Org}(\text{sol})$ and $\text{Org}(\text{ads})$ are organic molecules in the aqueous media that adsorbed on the adsorbent, respectively. x is the number of H_2O molecules replaced by one molecule of organic adsorbate. Attempts were made to fit experimental data to various isotherms including Temkin, Freundlich and Langmuir adsorption isotherms are tested. By far the results were best fitted Langmuir adsorption isotherm:

$$C/\theta = 1/K_{\text{ads}} + C \quad (9)$$

Here C is the concentration of inhibitor (g/L), K_{ads} is the adsorption-desorption equilibrium constant and θ is the surface coverage. Plots of C/θ against C yield straight lines as shown in Fig.8 and the corresponding linear regression parameters are listed in Table 4. It is evident that linear correlation coefficient (R^2) are almost equal to 1 and the slope values are also close to 1 which indicates the adsorption of BPDO on mild steel surface abide Langmuir adsorption isotherm in 1M HCl solutions. From the intercept of the straight lines, the values of K_{ads} were calculated and are summarized in Table 4. The standard free energy of adsorption (ΔG_{ads}) is calculated using the following equation:

$$\Delta G_{\text{ads}} = -RT \ln (55.5 \times K_{\text{ads}}) \quad (10)$$

The value 55.5 in the above equation is the molar concentration of water in solution in mol/L. R is the universal gas constant and T is the thermodynamic temperature. It is found that the values of K_{ads} decrease when temperature increases. It shows that the interaction between the metal surface and the adsorbed molecules are weakened resulting in the easy removal of the inhibitor molecules. Data of this kind go on to explain the reduce in the inhibition efficiency when temperature increases. In the present study, the calculated value of ΔG_{ads} around -20 kJ/mol, confirmed that BPDO spontaneously adsorbed on mild steel surface through physical adsorption mechanism. Generally, the value of ΔG_{ads} around -20 kJ/mol or lower indicates the electrostatic interaction between charged metal surface and charged molecules in the bulk of the solution while those around -40 kJ/mol or higher involves charge sharing or charge transfer between the metal surface and organic molecules [30]. The following two cases explain the dependence of ΔG_{ads} on temperature [31]:

- (i) T increases with increase in ΔG_{ads} (become less negative) which confirms the occurrence of exothermic process.
- (ii) T increases with decrease in ΔG_{ads} (become more negative) which indicates the occurrence of endothermic process.

The standard adsorption enthalpy (ΔH_{ads}) is calculated using the van't Hoff equation:

$$\ln K_{\text{ads}} = -\Delta H_{\text{ads}}/RT + \text{constant} \quad (11)$$

Figure 9 shows the plot of $\ln K_{\text{ads}}$ vs $1/T$ and slope is equal to $-\Delta H_{\text{ads}}/R$. Standard entropy of adsorption (ΔS_{ads}) is calculated using thermodynamic basic equation

$$\Delta G_{\text{ads}} = \Delta H_{\text{ads}} - T\Delta S_{\text{ads}} \quad (12)$$

The inference that the adsorption of BPDO is an exothermic process is indicated by the negative sign of ΔH_{ads} . Considering the absolute value of ΔH_{ads} , physisorption is distinguished from chemisorptions is an exothermic process.

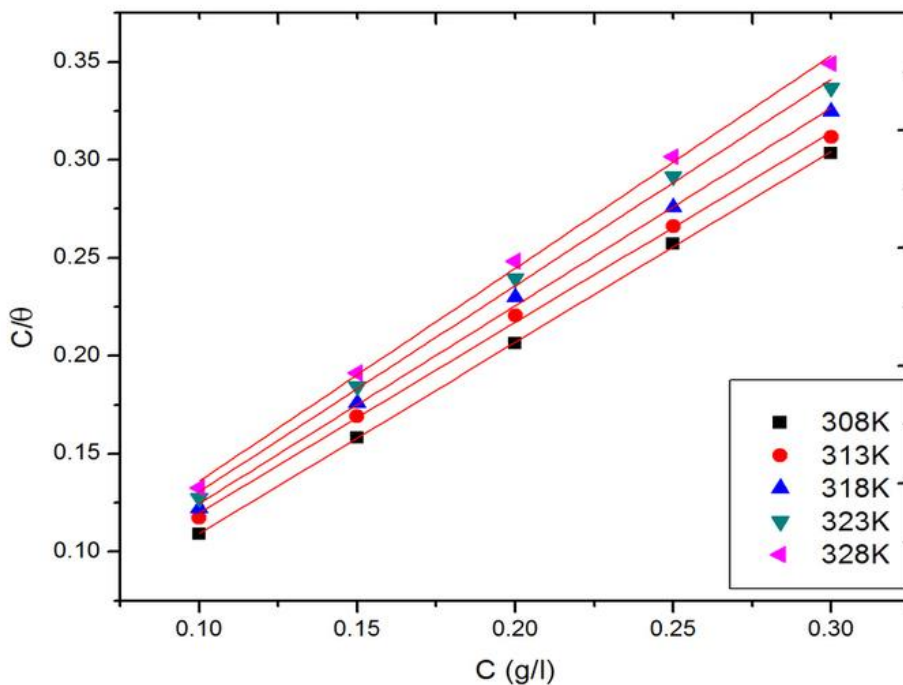


Figure 8. Langmuir adsorption models of BPDO on mild steel in 1 M HCl at 308 – 328K

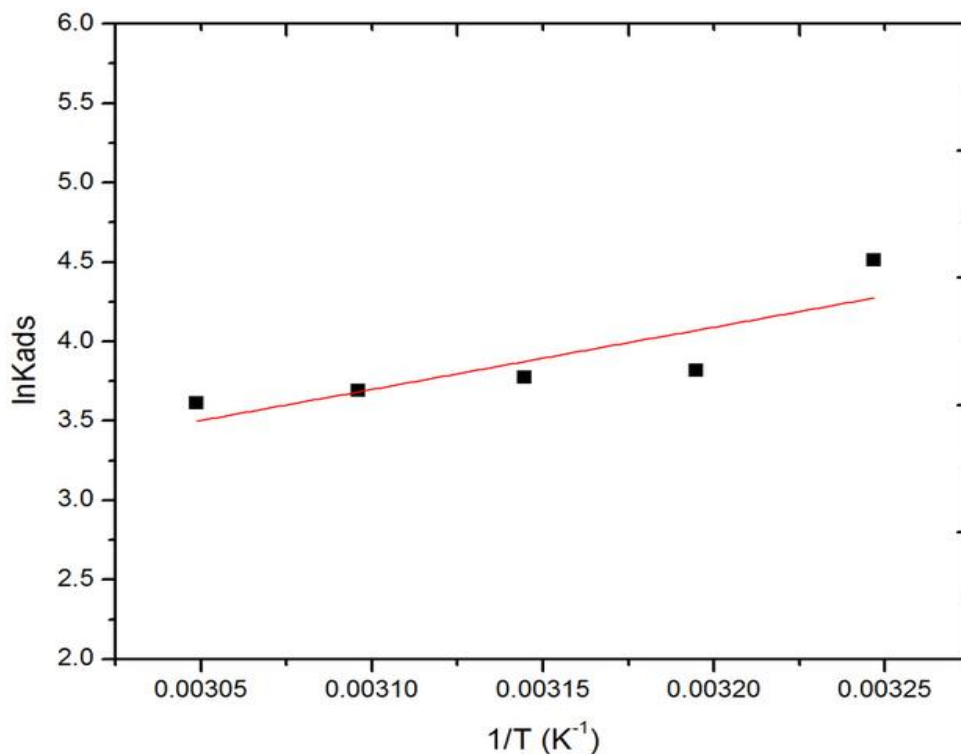


Figure 9. Straight lines of $\ln K_{ads}$ versus $1/T$ for the adsorption of BPDO at mild steel/ HCl.

The enthalpy of adsorption is lower than 40kJ/mol for physisorption process while for chemisorptions process, the enthalpy of adsorption approaches 100 kJmol^{-1} [30]. In the present case, the absolute value of ΔH_{ads} for adsorption of BPDO are ranged from -35.03 to -39.10 kJ/mol (Table 4),

which is lower than 40kJ/mol and indicates that physisorption takes place [32,33]. A decrease in entropy is the result when the values of entropy of adsorption are negative and large as the inhibitor molecules move freely in the bulk solution and adsorb in an orderly fashion on the mild steel. In the more, according to thermodynamic principles, as adsorption is an exothermic process, a decrease in entropy should accompany it.

Table 4. Langmuir adsorption isotherm for mild steel in 1M HCl solutions in the presence of BPDO.

Temperature (K)	K_{ads} (L/mol)	$-\Delta G_{\text{ads}}$ (kJ/mol)	ΔH_{ads} (kJ/mol)	$-\Delta S_{\text{ads}}$ (J/mol/K)	R^2
308	90.90	21.83		35.03	0.999
313	45.45	20.38		39.10	0.998
318	43.47	20.59	-32.62	37.83	0.998
323	40.00	20.69		36.94	0.997
328	37.03	20.80		36.04	0.998

3.6. X-ray Diffraction Analysis

The metal and metal oxide phases were investigated by X-ray diffraction techniques and corresponding XRD patterns of the surface of the mild steel specimens immersed in HCl solution are given in Fig.10.

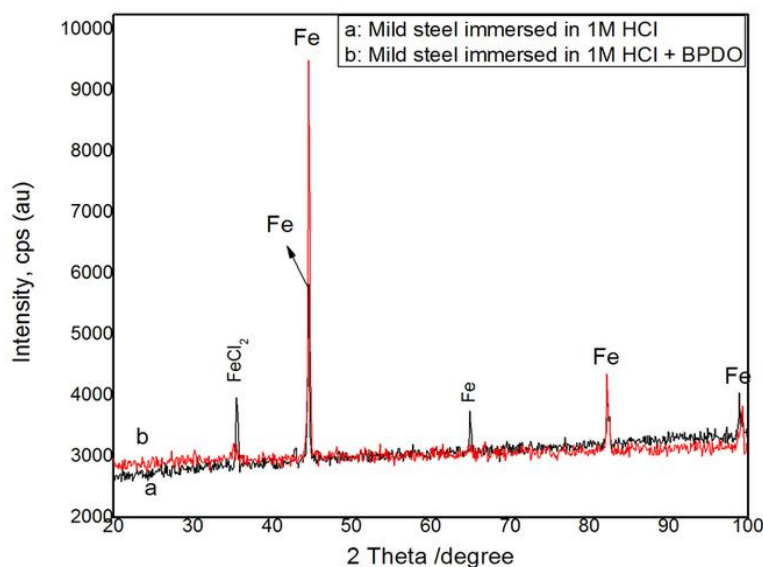


Figure 10. XRD patterns of mild steel exposed in 1M HCl (a) and presence of BPDO (b).

The patterns obtained clearly reveal the presence of metal and metal oxide phases. A series of characteristics peaks at 35.4 (104), 45.4 (110), 64.7 (200), 82.5 (211) and 99 (220) is observed and they are accordance with the standard Fe and FeCl₂ pattern (JCPDS: 06-0696). Peak at $2\theta = 35.4^\circ$ can be assigned to chlorides of iron. The peak due to iron appears at $2\theta = 45.4^\circ, 64.7^\circ, 82.5^\circ$ and 99° .

(Fig.10a), It is seen here that the surface of the metal immersed in 1M HCl alone contains FeCl_2 . Figure 10b shows X-ray diffraction patterns of mild steel immersed in 1M HCl solutions containing 300mg/l of BPDO. No brown film observed visually. The peaks due to iron appeared at $2\theta = 45.4^\circ$, 64.7° , 82.5° and 99° , which indicated the absence of oxides of iron and iron chloride (FeCl_2 , Fe_2O_3 , Fe_3O_4 and FeOOH). From the observations, it is clearly reflected that the formation of a barrier layer on the surface of mild steel in the presence of BPDO.

3.7. Analysis of FT-IR Spectra

The FTIR spectrum of pure BPDO is given in Fig.11a. Appearance of bands at 3057 cm^{-1} and 2864 cm^{-1} are due to the presence of C-H stretching vibrations in aromatic ring. A sharp band at 1642 cm^{-1} is due to C=O stretching of BPDO. The bands appeared at 1448 and 1321 cm^{-1} in FT-IR spectrum are assigned to C-C and C-H stretching vibrations. The C-H in-plane bending vibrations of the present compound identified at 1180 and 1151 cm^{-1} in FT-IR spectrum. Aromatic out of plane bending stands for the group of peaks appears between 900 cm^{-1} and 600 cm^{-1} . Fig.11b shows the FT-IR spectrum of the surface film on mild steel specimen after 2 h immersion in 1M HCl containing 300 mg/l of BPDO. All the peaks observed for BPDO powder are also noticed for the surface film of the BPDO on the mild steel surface, which means that most of the functional groups within BPDO are also present in the adsorbed surface film. The main difference between both spectra is that the presence of BPDO on mild steel exhibits peaks somewhat subdued intensities and vanished in the adsorbed surface films. The peak at 3381 cm^{-1} is transferred to 3353 cm^{-1} . These observations prove to be strong evidence in favor of the BPDO has synchronized with Fe^{2+} through lone pair electrons in oxygen atom and also through the pi electrons of benzene ring which results the formation of Fe^{2+} -BPDO complex on the anodic sites of the mild steel surface.

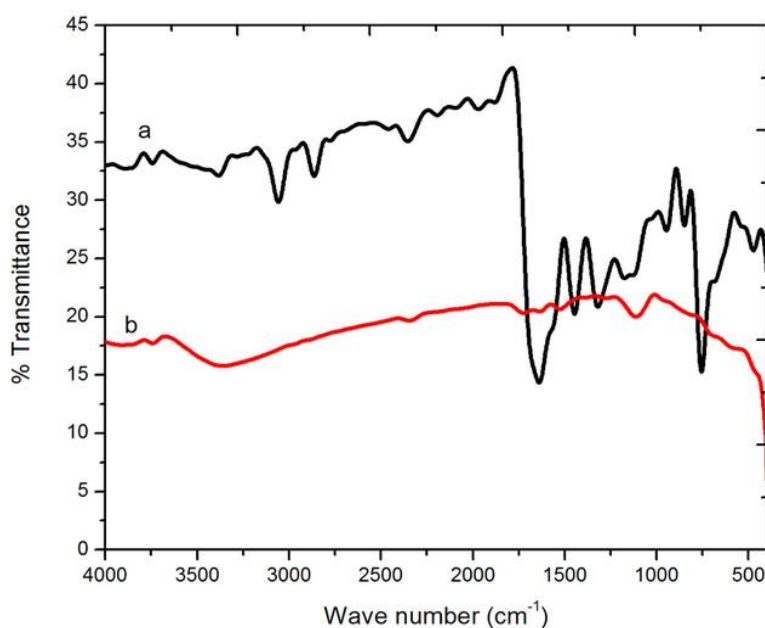


Figure 11. FT-IR spectra of BPDO (a) and BPDO adsorbed on the mild steel surface (b)

3.8. SEM and EDX investigations

Both SEM and EDX experiments are carried out to find whether the BPDO molecules are adsorbed on the mild steel surface. Fig 12a shows the SEM micrographs of mild steel surface immersed in 1M HCl solutions. The specimen was highly damaged in 1M HCl solution which shows the corrosion of mild steel in 1M HCl. Fig 12b illustrate that in the presence of 300 mg/l of BPDO in 1M HCl solution, the surface coverage increases which in turn results in the formation of insoluble complex on the surface of the metal (Fe^{2+} - BPDO). These images suggest that the inhibitor system creates a thin protective film, which inhibits the mild steel dissolution.

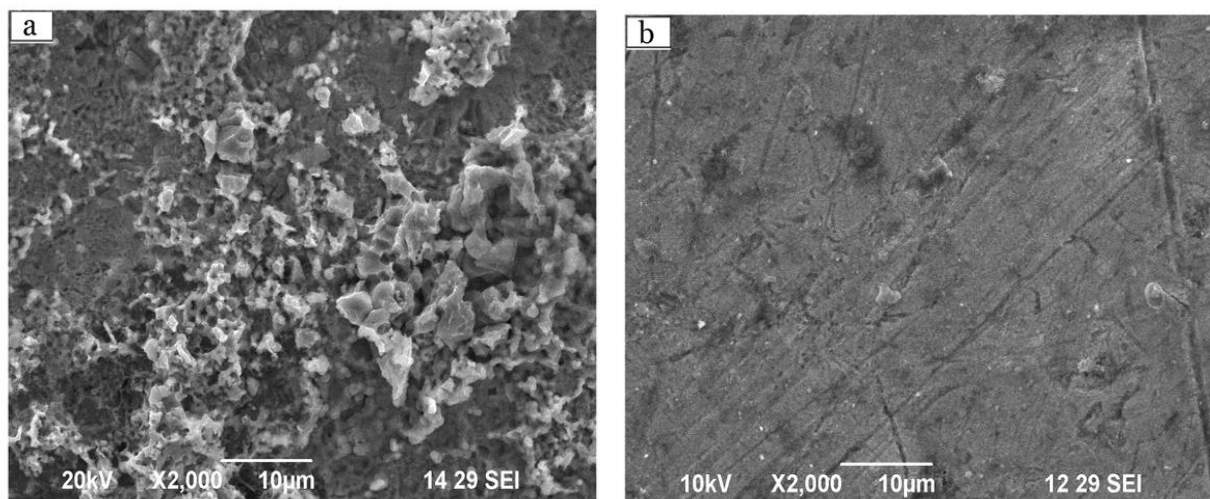


Figure 12. Scanning electron micrograph of a) Mild steel immersed in 1M HCl and b) BPDO deposited on mild steel surfaces.

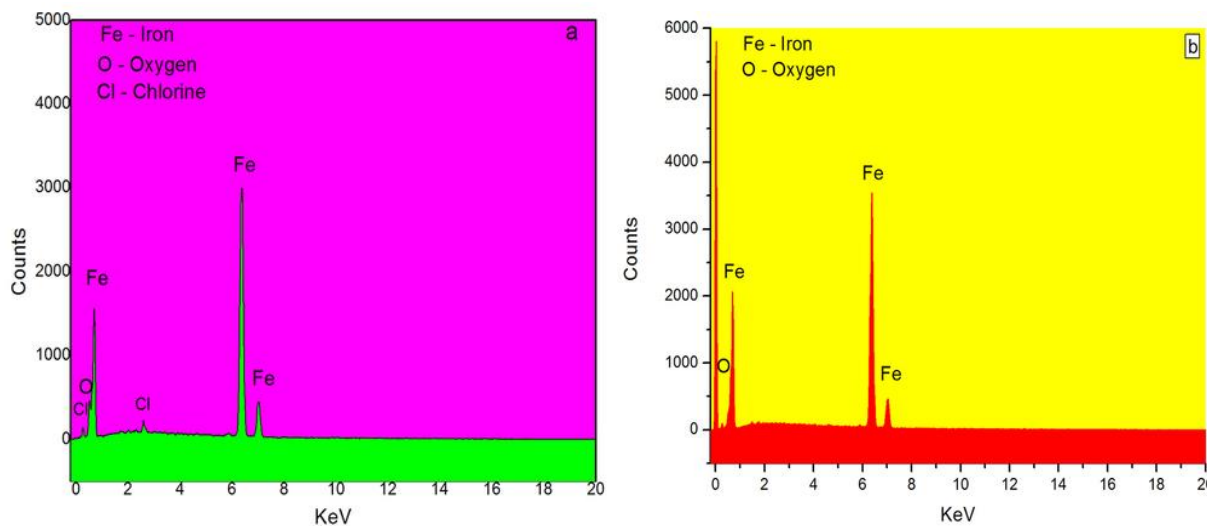


Figure 13. a) EDX spectra of mild steel in 1M HCl b) EDX spectra of BPDO film deposited on mild steel surfaces.

EDX spectrums were recorded for mild steel specimens exposed for 2 h in 1M HCl solution in the absence and presence of 300 mg/l concentration of BPDO. In absence of BPDO compound, the EDX spectrum (Fig.13a) shows the characteristic peaks of some elements (Fe and O with small quantities of Cl) constituting the mild steel specimens. These peaks could have arisen from the formation of iron chlorides and iron oxides by attack of aqueous hydrochloric acid solution on mild steel. In the presence of BPDO compound (Fig.13b), the EDX spectra did not show additional lines. However, the iron peak significantly enhanced upon adding BPDO compound to 1M HCl solution. This enhancement of iron peak is due to adsorption of BPDO over mild steel surface as thin layer. This layer is undoubtedly due to the inhibitor. The percentage of atomic contents of elements on the mild steel surface after exposure to 1M HCl solution with and without BPDO is tabulated in Table 5.

Table 5. EDX analysis of mild steel in 1M HCl and containing optimum concentration of BPDO

Medium	Composition		
	Fe	O	Cl
1 M HCl (a)	73.64	22.79	3.57
BPDO (b)	94.75	5.25	-

3.9. Quantum Chemical Studies

The quantum chemical calculations are very useful for studying corrosion inhibition mechanism. The frontier molecular orbital theory plays a vital role in the prediction of adsorption centers of the organic molecules that are responsible for the interaction with surface metal atoms. The design and development of organic compounds as corrosion inhibitors for protecting metals against corrosion is the most practical methods, the important tools are the quantum chemical parameters like E_{HOMO} and E_{LUMO} . The energy gap (ΔE) is calculated using the relationship:

$$\Delta E = (E_{\text{HOMO}} - E_{\text{LUMO}}) \quad (13)$$

Past studies reported that good corrosion inhibitors who not only donate electrons to empty orbital of the metal, but also accept free electrons from the metal [34]. Fig. 14, 15 and 16 show HOMO, LUMO and the optimized molecular structure of BPDO respectively. Table 6 shows the values of E_{HOMO} , E_{LUMO} , ΔE , ionization potential, dipole moment, electron affinity and ΔN computed using AM1 method. The study revealed that the BPDO had high HOMO and low LUMO. The inclination of the molecule to supply electrons to compatible acceptor molecules with low energy molecular orbital is indicated by the high values of E_{HOMO} . The low values of E_{LUMO} indicated an ability of accepting electrons to molecule, which could facilitate the adsorption and therefore improved inhibition efficiency resulted [35, 36].

Quantum chemical calculations have increasingly used for the prediction of molecular properties and to provide qualitative explanation for several findings in many areas of chemistry and biology [37, 38]. The success of these calculations relied on its better accuracy achieved at a relatively

low computational cost and due to the formulation of reactivity parameters such as Fukui function, chemical hardness, electro negativity, softness etc. These parameters are most important to determine corrosion mechanism.

Table 6. Quantum chemical parameters for BPDO

Calculated parameters	Value
E_{HOMO} (eV)	-0.2729
E_{LUMO} (eV)	-0.1354
ΔE ($E_{\text{HOMO}}-E_{\text{LUMO}}$) (eV)	0.1375
Dipole moment(D)	0.3075
Ionization Potential (eV)	0.2729
Electron affinity(eV)	0.1354
Molecular weight(amu)	324.00
ΔN	2.4729

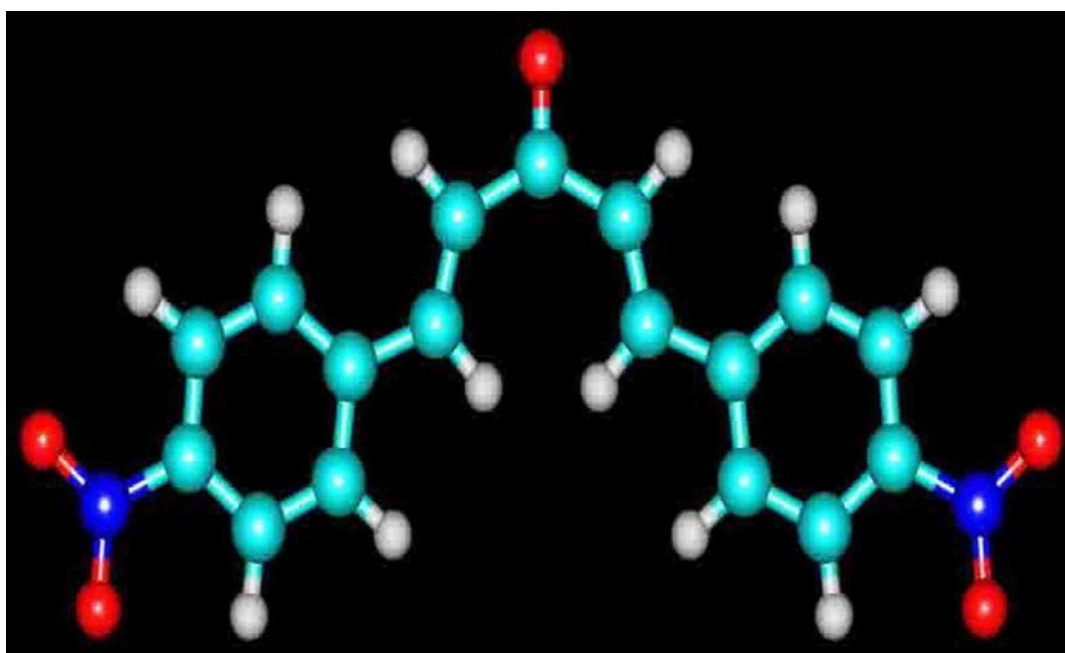


Figure 14. Optimized molecular structure of BPDO

According to Pearson approximation [39], chemical hardness (η) and electronegativity (χ) are related to electron affinity (A) and Ionization potential (I) as:

$$\chi = I + A/2 \quad (14)$$

$$\eta = I - A/2 \quad (15)$$

Ionization potential and electron affinity values have been used to calculate absolute chemical hardness and electro negativity [40]. E_{HOMO} and E_{LUMO} are directly related to the ionization potential (I) and the electron affinity (A) as:

$$I = - E_{\text{HOMO}} \quad (16)$$

$$A = -E_{\text{LUMO}} \quad (17)$$

Using a theoretical χ value of 7 eV/mol according to Pearson's electro negativity scale [41] and a global hardness η value of 0 eV/mol for Fe, the fraction of electrons transferred, ΔN is given as [42]:

$$\Delta N = [5 - (2 E_{\text{HOMO}} - \Delta) / 2] / \Delta \quad (18)$$

According to Lukovits [43], if ΔN is greater than 3.6, the protection efficiency decreases with enhancing electron donating ability at the metal surface and if $\Delta N < 3.6$, the protection efficiency increases. More precise is the wording "electron donating ability" than the expression "fraction of electrons transferred", which does not imply that the figures of ΔN shows the number of electrons departure the donor and entering the acceptor molecule.

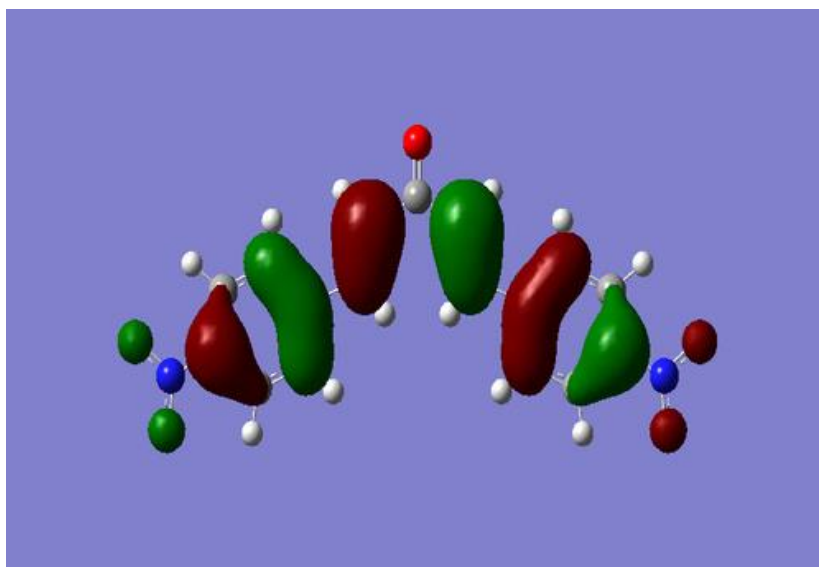


Figure 15. The highest occupied molecular orbital (HOMO) of the BPDO

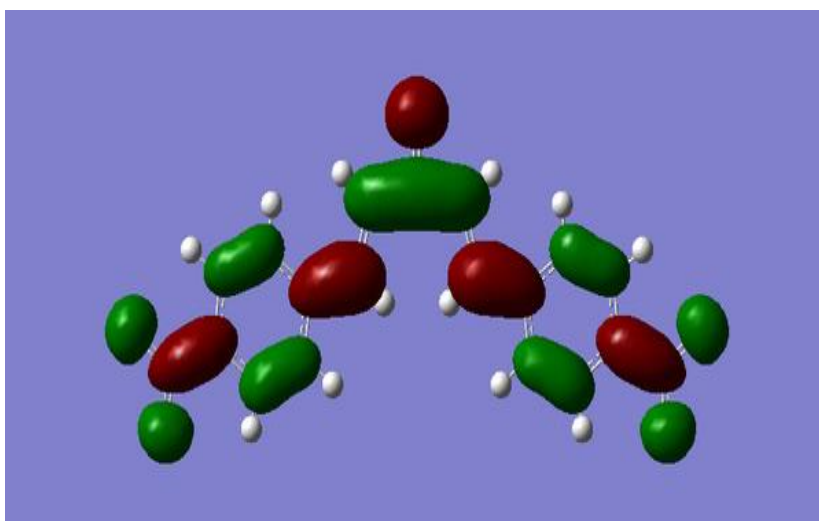
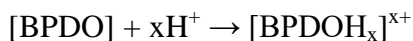


Figure 16. The lowest unoccupied molecular orbital (LUMO) of the BPDO

Therefore the values of these quantities indicate trends within a set of molecules, but their absolute value might not correspond to reality. With respect to this study, the supplier (donor) of electrons was BPDO and the acceptor was the mild steel surface. Thus, it is proved that, only on the basis of the interactions between the donor and the acceptor, the adsorption of inhibitor occurred on the mild steel surface.

3.10. Explanation of Corrosion Inhibition

The data obtained from weight loss measurements and different electrochemical measurements, it is concluded that by adsorption of metal solution interface, the BPDO inhibits the corrosion of mild steel in 1M HCl. Generally it is assumed that the initial step in the mechanism of the inhibitor action is the adsorption of organic molecules at the metal surface interface. Adsorption of organic molecules on the metal surface is possible in four ways [44]. In the present study, BPDO molecules possess electron rich NO₂ group, O atoms and aromatic ring which favor the adsorption on mild steel surface. Therefore, the possible reaction centers are unshared electron pair of O atoms and pi-electrons of aromatic ring in the BPDO molecules. From the experimental and theoretical point of view, it is confirmed that the BPDO can directly adsorb on the iron surface by replacing the adsorbed species which occur on the basis of donor- acceptor interactions between the lone pairs of the oxygen atoms, delocalized pi-electrons of the benzene ring in BPDO molecule and the vacant d-orbitals of iron atoms. The adsorption of BPDO in 1M HCl solution can be explained as follows. BPDO might be protonated in the hydrochloric acid solution as



The BPDO may exist as protonated species in an acidic solution. In addition, the evolution of hydrogen is diminished when protonated BPDO adsorb on the cathodic sites of mild steel surface. Although, BPDO molecules contain electron donating groups like Oxygen atoms and delocalized pi electrons in aromatic rings that are able to coordinate with iron at anodic sites. Anodic dissolution of mild steel may decrease when adsorption of BPDO on anodic sites takes place.

4. CONCLUSION

BPDO is a precious organic inhibitor for the acid corrosion of mild steel and the protection efficiency enhances with raise in the BPDO concentration. Effect of temperature results show that the decrease of inhibition efficiency with rise in temperature and the higher value of E_a in presence of BPDO can be interpreted as physisorption. Thermodynamic and kinetic data reveal that the BPDO follow the physical adsorption mechanism on mild steel surface in 1M HCl solutions. Tafel polarization studies indicated that BDPO act as a mixed type inhibitors, but predominantly acted as anodic inhibitors. Electrochemical impedance measurements show the formation of a protective film on the mild steel surface in 1M HCl. FT-IR data clearly indicate that the barrier layer consists of Fe-BPDO complex. The morphology of mild steel surface in the presence of BPDO show the smooth surface indicating the protective action of the BPDO in 1M HCl medium. XRD spectra show that the iron and iron oxide phases in the presence and absence of BPDO. The results inferred clearly indicate

that when there is increase in E_{HOMO} , BPDO also increased and simultaneously, the decrease in $E_{\text{LUMO}} - E_{\text{HOMO}}$ is also noticed. It is also proved that the most probable sites for bonding the mild steel surface by offering electron to iron are the areas that contain oxygen atoms.

References

1. R. Karthik, G. Vimaladevi, S.M. Chen, A. Elangovan, B. Jeyaprabha and P. Prakash, *Int. J. Electrochem. Sci.*, 10 (2015) 4666.
2. S. Velrani, P. Muthukrishnan, B. Jeyaprabha and P. Prakash, *International Journal of Engineering Research and Technology.*, 3 (2014) 2704.
3. R. Karthik, P. Muthukrishnan, A. Elangovan, M. M. Sri Vidhya, B. Jeyaprabha and P. Prakash, *Prot. Met. Phys. Chem.*, 51 (2015) 667.
4. J.G.N. Thomas, Proc of the 5th European Symp. On corrosion inhibitor, Ann.Univ. Ferrara, Italy, N.N. Sez V, Supl.N.8 (1980) 453.
5. R. Solmaz, E. Altunbas and G. Kardas, *Mater. Chem. Phys.*, 125 (2011) 796.
6. A. Popova, M. Christov and A. Zwetanova, *Corros. Sci.*, 49 (2007) 2131.
7. L. Xianghong, D. Shuduan, H. Fu and L. Taohong, *Electrochim. Acta.*, 54 (2009) 4089.
8. W.H. Li, Q. He, S.T. Zang, C.L. Pei and B.R. Hou, *J. Appl. Electrochem.*, 38 (2008) 289.
9. L. Herrag, A. Chetouani, S. Elkadiri, B. Hammouti and A. Aouniti, *Port. Electrochimica Acta.*, 26 (2008) 211.
10. G.Y. Elewady, *Int. J. Electrochem. Sci.*, 3 (2008) 1149.
11. N. Caliskan and E. Akbas, *Mater. Chem. Phys.*, 126 (2011) 983.
12. D.K. Yadav, B. Maiti and M.A. Quraishi, *Corros. Sci.*, 52 (2010) 3586.
13. P. Muthukrishnan, B. Jeyaprabha, P. Tharmaraj and P. Prakash, *Res. Chem. Intermed.*, 41 (2015) 5961.
14. K. Laarej, M. Bouachrine, S. Radi, S. Kertit and B. Hammouti, *E. J. Chem.*, 7 (2010) 419.
15. V. Sedighi, P. Azerang and S. Sardari, International conference on advances in Biological and Pharmaceutical sciences, (ICABPS'2012) March 24-25 (2012) Dubai.
16. A. Singh, I. Ahamad, V.K. Singh and M.A. Quraishi, *J. Solid. State. Electr.*, 11 (2011) 1087.
17. I.B. Obot and N.O. Obi-Egbedi, *Corros. Sci.*, 52 (2010) 282
18. D.K. Yadav and M.A. Quraishi, *Ind. Eng. Chem. Res.*, 51 (2012) 14966.
19. M.A. Quraishi, I. Ahamed and R. Prasad, *Corros. Sci.*, 52 (2010) 1472
20. A. Jamal Abdul Nasser, M. Anwar Sathiq, *Arabian J. Chem.*, doi.org/10.1016/j.arabjc.2012.07.032.
21. M.A. Quraishi, A. Singh, V.K. Singh, D.K. Yadav and A.K. Singh, *Mater. Chem. Phys.*, 122 (2010) 114
22. H. Cang, W. Shi, J. Shao and Q. Xu, *Int. J. Electrochem. Sci.*, 7 (2012) 3726.
23. A.K. Singh, S. Khan, A. Singh, S. M. Quraishi, M. A. Quraishi and E.E.Ebenso, *Res Chem. Intermed.*, 39 (2013) 1191-1208
24. A. Ouchriff, M. Zegmout, B. Hammouti, S. El-Kadiri and A. Ramdani, *Appl. Surf. Sci.*, 252 (2005) 339.
25. W.J. Lorenz and F. Mansfeld, *Corros. Sci.*, 21 (1981) 647
26. P. Singh, M.A Quraishi and E.E.Ebenso, *Int. J. Electrochem. Sci.*, 7 (2012) 12270.
27. I. Ahamad, R. Prasad and M.A. Quraishi, *Corros. Sci.*, 52 (2010) 3033.
28. A. Doner and G. Kardas, *Corros. Sci.*, 53 (2011) 4223.
29. N. Gunavathy and S.C. Murugavel, *E. J. Chem.*, 9 (2012) 487.
30. P. Muthukrishnan, R. Karthik, B. Jeyaprabha and P. Prakash, *Int. J. Miner. Metall. Mater.*, 21 (2014) 1.
31. M. Gopiraman, P. Sakunthala, D. Kesavan, V. Alexramani, I.S. Kim and N. Sulochana, *J. Coat. Tech. Res.*, 9 (2012) 15.

32. M.J. Bahrami, S.M.A. Hosseini and P. Pilvar, *Corros. Sci.*, 52 (2010) 2793.
33. E. Ebenso and I.B. Obot, *Int. J. Electrochem. Sci.*, 5 (2010) 2012.
34. P. Chao, Q. Liang and Y. Li, *Appl. Surf. Sci.*, 252 (2005) 1596.
35. F. Bentis, M. Traisnel, H.F. Hildebrand and M. Lagrenee, *Corros. Sci.*, 46 (2004) 2781.
36. N.O. Obi-Egbedi and I.B. Obot, *Corros. Sci.*, 52 (2010) 263.
37. R.G. Parr and W. Yang, *Annu. Rev. Phys. Chem.*, 46 (1995) 701.
38. W. Kohn, A.D. Becke and R.G. Parr, *J. Phys. Chem.*, 100 (1996) 12974
39. R.G. Pearson, *Proc. Natl. Acad. Sci. USA.*, 83 (1986) 8440
40. C.G. Zhan, J.A. Nichols and D.A. Dixon, *J. Phys. Chem. A.*, 107 (2003) 4184.
41. R.G. Pearson, *Inorg. Chem.*, 27 (1988) 734.
42. R.G. Pearson, *J. Am. Chem. Soc.*, 85 (1963) 3533.
43. I. Lukovits, E. Lalman and F. Zucchi, *Corrosion.*, 57 (2001) 3.
44. H. Shorky, M. Yuasa, I. Sekine, R. M. Issa, H.Y. E. Baradie and G. K. Gomma, *Corros. Sci.*, 40 (1998) 2173.

© 2016 The Authors. Published by ESG (www.electrochemsci.org). This article is an open access article distributed under the terms and conditions of the Creative Commons Attribution license (<http://creativecommons.org/licenses/by/4.0/>).